Production of Scandium-44m and Scandium-44g with Deuterons on Calcium-44: Cross Section measurements and Production Yield Calculations

C. Duchemin, Arnaud Guertin, Ferid Haddad, Nathalie Michel, Vincent Métivier

Production of Scandium-44m and Scandium-44g with Deuterons on Calcium-44: Cross Section Measurements and Production Yield Calculations

C. Duchemin[a], A. Guertin[a], F. Haddad[a,b], N. Michel[a,b], V. Métivier[a]

[a]SUBATECH, Ecole des Mines de Nantes, Université de Nantes, CNRS/IN2P3, Nantes, France
[b]GIP Arronax, 1 rue Aronnax, 44817 Saint-Herblain, France

Abstract

HIGHLIGHTS

- Production of Sc-44m, Sc-44g and contaminants.

- Experimental values determined using the stacked-foil technique.

- Thick Target production Yield (TTY) calculations.

- Comparison with the TALYS code version 1.6.

ABSTRACT

Among the large number of radionuclides of medical interest, Sc-44 is promising for PET imaging. Either the ground state Sc-44g or the metastable state Sc-44m can be used for such application, depending on the molecule used as vector. This study compares the production rate of both Sc-44 states, when protons or deuterons are used as projectiles on an enriched Calcium-44 target. This work presents the first set of data for the deuteron route. The results are compared with the TALYS code. The Thick Target production Yields of Sc-44m and Sc-44g are calculated and compared with the proton route for three different scenarios: the production of Sc-44g for conventional PET imaging, its production for the new 3 γ imaging technique developed at the SUBATECH laboratory and the production of the Sc-44m/Sc-44g in-vivo generator for antibody labelling.

---

1. Introduction

Nuclear medicine is a specialty involving the use of radionuclides for diagnosis as well as for therapy of cancers. In the last years, the Positron Emission Tomography (PET) diagnosis technique has been developed rapidly through the use of fluorine-18. At the same time, molecular therapy using new isotopes like Lu-177 has shown very promising results. In this case, the radionuclide must have a half-life which matches that of the vector distribution (peptide or antibody). The combination of imaging information and therapeutic use of radionuclides is called theranostic and allows to personalize the treatment to each patient. Indeed, the diagnosis test, done prior to the treatment, permits to follow and control the patient response to the injected radiopharmaceutical. It allows a better control of the targeting and increases the benefit/toxicity ratio as useless treatments on patients with no response to the diagnosis test are avoided. For a better description of the tracer biodistribution, pairs of radionuclides of the same element are preferable.

Scandium is an useful element for this theranostic concept. Scandium-47 can be used for therapy while Sc-43 and Sc-44 can be used for Positron Emission Tomography (PET). Scandium-47 is a β- emitter (100%) with a half-life of $T_{1/2}$= 3.3492 days which decays to Ti-47. Its β energy makes it well suited for radionuclide therapy. Associated to its decay, a 159 keV γ-ray is emitted (branching ratio of 68 %) which can be used for imaging in Single Photon Emission Computed Tomography (SPECT). This isotope can be produced efficiently in nuclear reactor (Muller C. et al, 2014).

Scandium-43, with a half-life of 3.9 hours, is a β+ emitter with a branching ratio of 88.1%. Its production is quite difficult using accelerator since it needs expensive Ca-43 enriched target (Majkowska-Pilip and Bilewicz, 2011). Scandium-44 ground state, scandium-44g or Sc-44g, with a half-life of 3.97 hours, is also a β+ emitter (branching ratio of 94 %). This radioisotope can be produced via a generator system Ti-44/Sc-44g (Roesch et al., 2012) but also directly via the irradiation of an enriched Calcium-44 target (Muller C. et al, 2014, Alliot et al., 2015). Scandium-44g has an important production advantage over scandium-43 because the starting material, Ca-44, is more

2

abundant (2.1 %) than Ca-43 (0.14 %) leading to less expensive target material. Sc-44g is complementary to other PET isotopes. Indeed, the Sc-44g half-life is between that of Ga-68 ($T_{1/2}$ = 67.71 min) and Cu-64 ($T_{1/2}$ = 12.701 h).

Associated to Sc-44g decay, a high energy gamma ray at 1.157 MeV, with a high probability of occurrence (99.9 %), is emitted. This γ ray can be used in addition to the two 511 keV resulting from the positron annihilation, on the new three-gamma imaging technique developed at the SUBATECH laboratory (Nantes, France). The aim of this technique is to measure, on an event by event basis, the emitter location in three dimensions as proposed by Grignon C. et al., 2007. To do that, it is necessary to combine the line of response obtained with the two gammas following the positron/electron annihilation with the arrival direction of the third gamma emitted by the radio-isotope. A first device using liquid xenon as detection medium has been developed to show the feasibility of this new technique, called XEMIS for XEnon Medical Imaging System. Simulations have shown the possibility to reduce the injected dose to the patient with a good energy and spatial resolution (Oger et al., 2012). Today, an experimental device is in construction for the small animal imaging, named XEMIS 2 (Gallego Manzano et al., 2014).

Last but not least, with scandium-44, it is possible to match the half-life of the isotope to the vector characteristics. The 3.97 hours half-life of Sc-44g is well suitable for the use of peptide and small molecule with rapid distribution on the body. For long biological processes like the ones induced when antibodies are used, its metastable state, Sc-44m, can be used as an in-vivo generator of Sc-44g. This excited state of scandium has a half-life of 58.6 hours and decays mainly by Internal Transition (IT) to its ground state Sc-44g. It has been shown that when a molecule is labeled with Sc-44m, the Sc-44g formed by its decay remains attached to this molecule (Huclier-Markai et al., 2014). Sc-44m cannot be formed through the Ti-44/Sc-44 generator. It can be produced, at the same time as Sc-44g, with particle accelerators interacting on Ca-44 enriched target. Experimental data exist on the production of scandium-44 using protons as projectiles on Ca-44 (Mitchell et al., 1982, Levkovskij et al.1, 1991 and Krajewski et al., 2013). They are in good agreement with the assessment given by the TALYS code version 1.6 (Koning and Rochman, 2012). From these cross section values, the thick target production yields (TTY) (See Section 2.3) have been calculated to be 23 MBq/μA.h for Sc-44m and 2.7 GBq/μA.h for Sc-44g at 30 MeV (See

figure 1).

In some cases, deuterons can be advantageously used for isotope production (Alliot et al., 2015). This is the case for Copper-64 production from Nickel-64 enriched target as well as for the production of Re-186g using a Tungsten-186 enriched target. In this latter case, 3.7 times more activity can be obtained with deuterons of 17.6 MeV than with protons at the same energy (Duchemin et al., 2015). In order to investigate the potential advantage in using deuterons and due to the lack of experimental data with deuterons as projectiles, we have used the TALYS code to get hints on the best production route between proton and deuteron. The TALYS results for the Ca-44(d,2n) reactions are plotted in figure 2. The TTY calculated from these theoretical values is 65 MBq/μA.h for Sc-44m and 2.3 GBq/μA.h for Sc-44g at 30 MeV, showing a ratio Sc-44m/Sc-44g 3.3 times higher using deuterons than protons for this energy.

The aim of this work is to experimentally determine the Sc-44g and Sc-44m production cross sections using deuterons on an enriched Ca-44 target in order to be able to calculate the associated production yields, and make a comparison with the proton route. Experimental data have been extracted up to 34 MeV for the Ca-44(d,2n)Sc-44m,Sc-44g reactions, using the stacked-foil technique and gamma-spectrometry, at the ARRONAX cyclotron. Some results on the production of K-42,43 and Sc-43 have been also obtained but not in all the targets as the main objective was to properly measure the activity of Sc-44m and Sc-44g. Based on these new data, three different scenarios for the production of Sc-44 have been defined depending on the aim of its use: the first one corresponds to the use of Sc-44g for PET imaging with small molecules as vectors. In this case, the production of the metastable state Sc-44m has to be limited. The second one corresponds to the use of Sc-44g for the new three-gamma imaging technique, developed at the SUBATECH laboratory (Nantes, France). In this case, Sc-43 and Sc-44m will generate background in the detection system as they don't have the third γ emission with the energy required. The third one corresponds to the use of the Sc-44m/Sc-44g in-vivo generator to follow long biological processes. In this case, it is necessary to maximize the Sc-44m production. All our results are compared with the results of the TALYS code version 1.6, as these information were used to infer the potential interest of deuterons over protons.
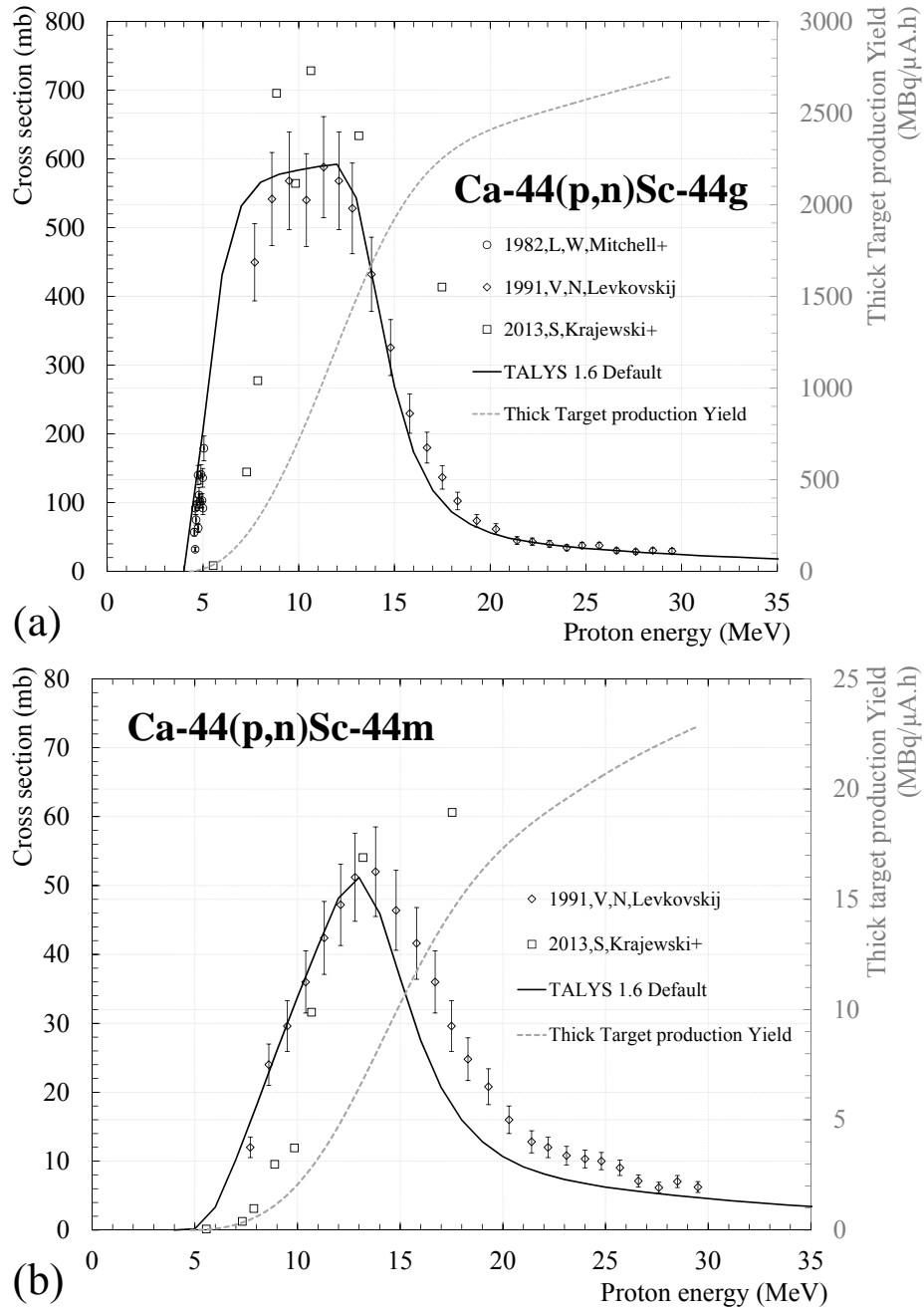
Figure 1: Experimental excitation functions for the Ca-44(p,n)Sc-44g (a) and Ca-44(p,n)Sc-44m (b) reactions with their calculated thick target production yield, compared with TALYS 1.6 with default models
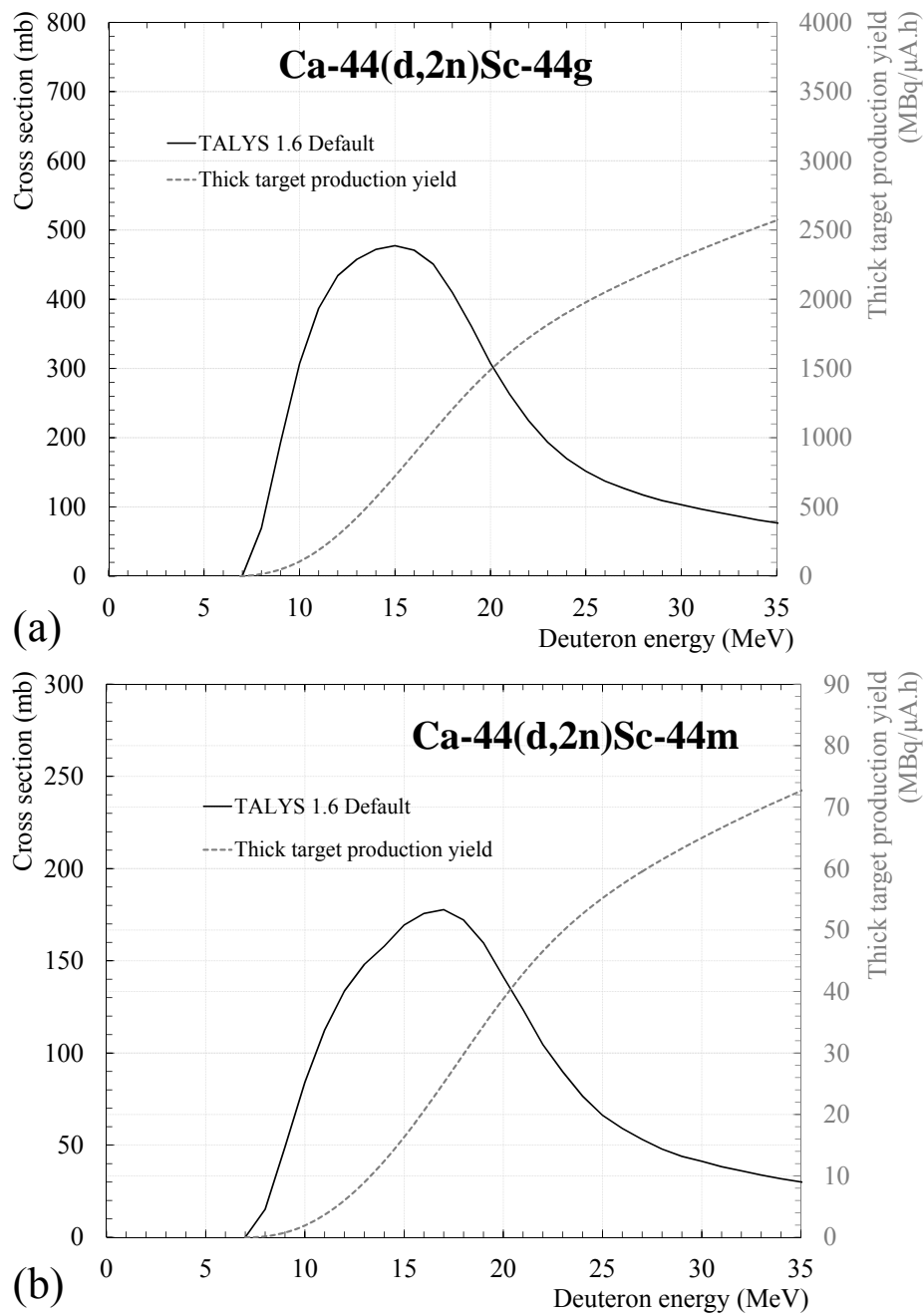
(a)

(b)

Figure 2: Estimations of the excitation functions of the Ca-44(d,2n)Sc-44g (a) and Ca-44(d,2n)Sc-44m (b) reactions from TALYS 1.6 with default parameters and the associated thick target production yield

2. Materials and methods

2.1. Experimental set-up

In this work, Sc-44g and Sc-44m are produced using an enriched Ca-44 carbonate target (CaCO$_3$) from Chemgas$^{®}$. The isotopic composition of the calcium powder is reported in Table 1.

Table 1: Isotopic composition of the calcium carbonate powder from Chemgas$^{®}$

Isotope	Ca-40	Ca-42	Ca-43	Ca-44	Ca-46	Ca-48
%	0.92	0.02	0.01	99.04	≤ 0.01	0.01

99.04 % of the calcium target is composed by Ca-44. Ca-40 represents the vast majority of the other Ca isotopes present in the target with 0.92 %. All isotopes investigated in this work are not produced from Ca-40. The parasitic reactions are on Ca-43 and Ca-42. Sc-44 is produced via Ca-44(d,2n) and Ca-43(d,n) reactions. The contribution on this latter isotope is negligible since Ca-43 is present at a level of only 0.01 %. The same holds for the production of Sc-43 which can be made via Ca-44(d,3n), Ca-43(d,2n) or Ca-42(d,n) (0.02 %). Both Ca-43 and Ca-42 are present at a low level in the target and their contribution can be neglected. Same comments can be made for the production of K-42 and K-43. The calcium carbonate targets have been prepared at the Institut de Physique Nucléaire dOrsay (IPNO, France) by the CACAO (Chimie des Actinides et Cibles radioActives à Orsay) project team (Petitbon-Thévenet, 2010). The backing of our target was chosen to be 100 micrometers thick aluminum foils with a surface of 25*25 mm^2, manufactured by the Goodfellow Company$^{®}$. The backing surface was first prepared to be sufficiently rough to insure a good adhesion of the carbonate calcium deposit. Before use, each support was cleaned with isopropanol. To perform the centrifugation/sedimentation, the apparatus of the Centre de Spectrométrie Nucléaire et de Spectrométrie de Masse in Orsay (France) was used. The experimental process is exposed in the article of Durnez, Petitbon-Thévenet and Fortuna published in 2014. An amount of 6.53 mg of calcium carbonate powder was used to make each target. This value corresponds to 5.44 mg with 20% of losses during the process. One milliliter of a mix of both chloroform and polystyrene (17 g/l) as well as two milliliters of ethyl acetate were added to the powder. This mix is transferred to a bottle and placed in an ultrasonic bath for one hour to produce the good quality slurry. Then the solution was transferred to the centrifuge tube mounted with the backing. The tube with

slurry was placed in the centrifuge and was spun at 3 500 revolutions per minute during one hour. After completing the sedimentation, the excess of the solvent is removed and the target is left aside for polymerizing during twelve hours. At the end of the process, the amount of target material is defined by precise weighting. Typical values are 2.54 (12) mg.cm^{-2} for our 10 targets.

At the ARRONAX cyclotron (Haddad et al., 2008), the cross section measurements are made using the stacked-foil method (Duchemin et al., 2015, Blessing et al., 1995) which consists in the irradiation of a set of thin foils, grouped as patterns. Each pattern contains a target to produce the isotopes of interest, a thin aluminium cover to protect the calcium carbonate deposit, a monitor foil to have information on the beam current through the use of a reference reaction recommended by the International Atomic Energy Agency and a degrador to change the incident beam energy from one target foil to the next one. Each monitor, deposit protection and degrador foil has been weighed before irradiation using an accurate scale ($\pm$ 10^{-5}g) and scanned to precisely determine its area. The thickness is deduced from these values, assuming it is homogeneous over the whole surface. In this work, 10 μm thick titanium monitor foils and 100 to 500 μm thick aluminium degrador foils were irradiated. The titanium and aluminium foils, with a purity of 99.6 % and 99 %, respectively, were purchased from Goodfellow®.

The ARRONAX cyclotron delivers deuteron beams with an energy uncertainty of $\pm$ 0.25 MeV, as specified by the cyclotron provider using simulations. The beam line is under vacuum and closed using a 75 μm thick kapton foil. The stacks were located about 7 cm downstream in air. The energy through each foil has been determined in the middle of the thickness of the foil using the SRIM software (Ziegler et al., 2010). Energy loss in the kapton foil and air have been taken into account. All along the stack, depending on the number of foils, the energy uncertainty calculated using the SRIM software (Ziegler et al., 2010) increases up to $\pm$ 0.61 MeV due to the energy straggling (see Table 4). Three stacks were irradiated with a different incident energy in order to minimize this energy dispersion and cover the energy range from 34 MeV down to 8 MeV, which corresponds to the whole energy range of interest (see Table 2). Irradiations were carried out with a mean beam intensity between 54 to 68 nA during 30 minutes. The beam current through the target has been limited knowing that CaCO$_3$ can be affected by a thermal decomposition above 800 Celsius degrees. In the worst case, the maximal power to the target was 7 mW/cm^2 which is

not enough to decompose the calcium carbonate. Irradiation conditions are reported in Table 2.

Table 2: Irradiation conditions and energies estimated with SRIM

Beam energy (MeV)	<Intensity> (nA)	Energy points (MeV)			
34.00 (25)	54	33.33 (28)	29.45 (44)	25.11 (54)	21.66 (60)
20.50 (25)	55	19.51 (29)	17.33 (36)	14.91 (44)	12.17 (58)
16.90 (25)	68	10.71 (49)	8.40 (61)		

For all the experiments, the recommended cross section of the reaction Ti-nat(d,x)V-48 (Tárkányi et al., 2001) is used to obtain information on the beam current from the Ti monitor foils. This reaction is well known over the whole studied energy range. A Faraday cup was placed after the stack to collect charges and control the intensity during the irradiation. The cross section values obtained with this measurement are in agreement with those obtained using the monitor foil within 6.5 % in average. This difference is explained by the beam stop used to collect the beam current after the stack which has no electron suppression device. In the stacks, 20 μm aluminium foils were placed in front of the Ca-44 carbonate deposit, for protection. The activity on Ca-44 were determined measuring the target and the protection cover together. The activity measurements in each foils were performed using a high purity germanium detector from Canberra (France) with low-background lead and copper shielding. All foils were counted twice. The first measurements started the day after the irradiation during one hour, for all target, protection cover and monitor foils. The second ones were performed for a minimum of 24 hours (one day) and up to 60 hours (during the week-end), one week after the end of irradiation for the Ca-44 targets and after three weeks for the monitor foils, waiting for the complete decay of Scandium-48. Indeed, Sc-48 ($T_{1/2}$ = 43.67 (9) hours) has common gamma lines with the radioisotope of reference, Vanadium-48 ($T_{1/2}$= 15.9735 (25) days). Gamma spectra were recorded in a suitable geometry calibrated in energy and efficiency with standard Co-57,60 and Eu-152 gamma sources from LEA-CERCA (France). The full widths at half maxima were 1.04 keV at 122 keV (Co-57 γ ray) and 1.97 keV at 1332 keV (Co-60 γ ray). Samples were placed at a height of 19 cm from the detector in order to reduce the dead time and the effect of sum peaks. The dead time during the counting was always kept below 10%.

2.2. Data processing

The activity values of the produced radioisotopes were derived from the γ spectra and the nuclear decay data (National Nuclear Data Center; Ekström and Firestone, 2004) given in Table 3 using the Fitzpeak spectroscopy software (FitzPeaks Gamma Analysis and Calibration Software version 3.66). Knowing the precise thickness of the foil and the activity value of the produced isotope, its production cross section is calculated using the activation formula (1) with the appropriate beam current:

$$\sigma = \chi \cdot \frac{Act \cdot A}{\Phi \cdot N_a \cdot M \cdot (1 - e^{-\lambda t})} \tag{1}$$

In this equation, the production cross section σ of a radioisotope depends on its measured activity reported to the time at the end of irradiation (Act), its decay constant (λ), its atomic mass (A), its areal density (M), its chemical and isotopic purity (χ), the irradiation duration (t) and the beam current (Φ).

In our experiment, each target foil received the same beam current as the monitor foil that follows. It is then easier to use the relative equation (2) in which the knowledge of the beam current is no longer necessary. In this equation, the prime parameters are associated to V-48 while the others relate to the radioisotope produced in the target (i.e. Sc-44m, Sc-44g, Sc-43, K-42 and K-43).

$$\sigma = \sigma' \cdot \frac{\chi' \cdot Act \cdot A \cdot M' \cdot (1 - e^{-\lambda' t})}{\chi \cdot Act' \cdot A' \cdot M \cdot (1 - e^{-\lambda t})} \tag{2}$$

The cross section uncertainty is estimated with a propagation error calculation. Since all the parameters of equation (2) are independent, the total error is expressed as a quadratic sum (Eq.(3)). The main error sources come from the recommended cross section, the activity values of each produced radioisotopes and the foils thickness uncertainties. An uncertainty around 11% is applied to the recommended cross section values given by the uncertainty of the nearest experimental value. The uncertainties on the activity of the radio-isotopes produced on the Ca-44 targets depend on different parameters as the gamma line branching ratio and energy, half-life etc, described afterwards. These uncertainties are, in average, of 3.5 % for Sc-44m activity, 16 % for Sc-44g, 20 % for K-42, 18 % for K-43 activity and up to 30 % for Sc-43. The uncertainty on the activity of V-48 is 4 % in average. Around 1

% of uncertainty is calculated for the areal density. The contribution of the irradiation time uncertainty is not significant and has been neglected.

$$\frac{\Delta\sigma}{\sigma} = \sqrt{\left(\frac{\Delta\sigma'}{\sigma'}\right)^2 + \left(\frac{\Delta Act}{Act}\right)^2 + \left(\frac{\Delta Act'}{Act'}\right)^2 + \left(\frac{\Delta M}{M}\right)^2 + \left(\frac{\Delta M'}{M'}\right)^2} \quad (3)$$

2.3. Thick Target production Yield (TTY)

Using the cross section values obtained in this work or those in databases as a function of the energy $\sigma(E)$, we have calculated the associated Thick Target production Yields in Bq/μA.h, also called production yield or integral yield. The values are obtained as a function of the projectile energy, using the relation (4).

$$TTY = \Phi.\chi.\frac{N_a.\rho}{A}(1 - e^{-\lambda.t}) \int_{Emin}^{Emax} \frac{\sigma(E)}{\frac{dE}{dx}} dE \quad (4)$$

In relation (4), ϕ is set to be the number of particles per second delivered in one μA. χ corresponds to the isotopic and chemical purity of the target and N_a is the Avogadro number. The TTY results presented in this article are obtained using the density ρ and the atomic mass A of a calcium-44 carbonate target. The density is provided by the CACAO team who prepared the target and fixed at 2.71 g.cm^{-3}. All the TTY calculation is done taking into account one hour of irradiation, which is less that the time where the activity of the investigated radionuclides is saturated. $\frac{dE}{dx}$ is the specific energy loss of the projectile in the target material (MeV.cm^{-1}). In a thick target, the incident particle energy decreases with the penetration depth. E$_{max}$ corresponds to the incident projectile energy when it enters into the target whereas E$_{min}$ corresponds to its energy when it leaves the target. TTY is also called production yield or integral yield.

2.4. Comparison with the TALYS 1.6 code

In this work, all the experimental cross section values are compared with the latest version (1.6) of the TALYS code released in December, 2013 (Koning and Rochman, 2012). TALYS is a nuclear reaction program to simulate reaction induced by light particles on nuclei heavier than carbon. It incorporates theoretical models to predict observables including theoretical cross

section values as a function of the incident particle energy (from 1 keV to 1 GeV). A combination of models that better describes the whole set of data available for all projectiles, targets and incident energies have been defined by the authors of the code and put as default in the code. This way, the code can be launched with minimum information in the input file: the projectile type and its incident energy, the target type and its mass. The experimental data obtained in this work are compared to TALYS with default models (named TALYS 1.6 Default in the graphs).

3. Results and discussions

Production cross sections are needed to obtain the Thick Target production Yield for a produced radio-isotope. In a first part, new results on deuteron induced Sc-44 production cross section on Ca-44 will be exposed, as well as the contaminant cross sections. In a second part, the Sc-44m and Sc-44g TTY will be calculated and compared with proton routes for different production scenarios.

3.1. Production cross sections for deuteron induced reactions

The production cross sections of the produced radioisotopes are plotted in figures 3 to 7 as full circles and the associated numerical values are reported in Table 4.

3.1.1. Production cross section of Sc-44m

Sc-44m ($T_{1/2}$ = 58.6 (1) h) mainly decays by Internal Transition (IT), at 98.80 (7) %, to its ground state Sc-44g ($T_{1/2}$ = 3.97 (4) h) by emitting an intense γ ray at 271.13 keV (Table 3). It also decays by Electron Capture (EC) process (1.20 (7) %) to Ca-44 (stable) by emitting three γ rays of 1001.83 (1.20%), 1126.06 (1.20%) and 1157.031 keV (1.20%). The high branching ratio of the 271.13 keV gamma line allows to use it to extract the Sc-44m production cross section plotted in figure 3, with the results of the TALYS code version 1.6 with default parameters.

The Sc-44m production cross section shows a maximum at 17.3 MeV with a value of 185 mb (see figure 3). The TALYS code gives cross section values slightly shifted to lower energies as compared to those experimentally determined (see figure 2(a)). The magnitude of the cross section is of the same order for both experimental and TALYS results.
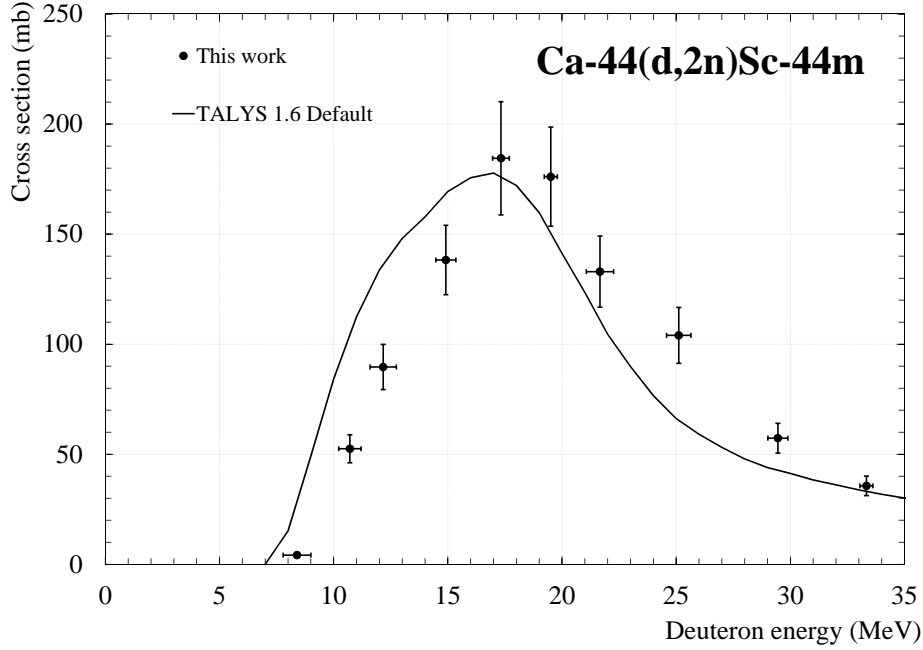
Figure 3: Excitation function for the Ca-44(d,2n)Sc-44m reaction

3.1.2. Direct production cross section of Sc-44g

Sc-44g ($T_{1/2}$ = 3.97 (4) h) is a 100 % EC/β+ emitter which decays to Ca-44 (stable). It emits an intense gamma ray at 1157.031 keV (99.9 %), used to determine its activity. The measured activity and the cross section obtained in this work correspond to the direct production of Sc-44g in a Ca-44 carbonate target. As Sc-44m decays to Sc-44g, its contribution has been determined and removed from the Sc-44g activity, as well as the contamination by the direct decay of Sc-44m to Ca-44 in the gamma line at 1157 keV, which is common to Sc-44m (I_γ = 1.2 %) and Sc-44g. The experimental Sc-44g production cross section is plotted in figure 4.

In figure 4, the experimental data show a peak broader with a maximum 10 % higher than the results obtained using the TALYS calculations. The maximum of the experimental cross section is found to be 538 mb at 14.9 MeV, against 470 mb with TALYS for the same incident deuteron energy. In this case, there is no energy shift between TALYS and the experimental results.
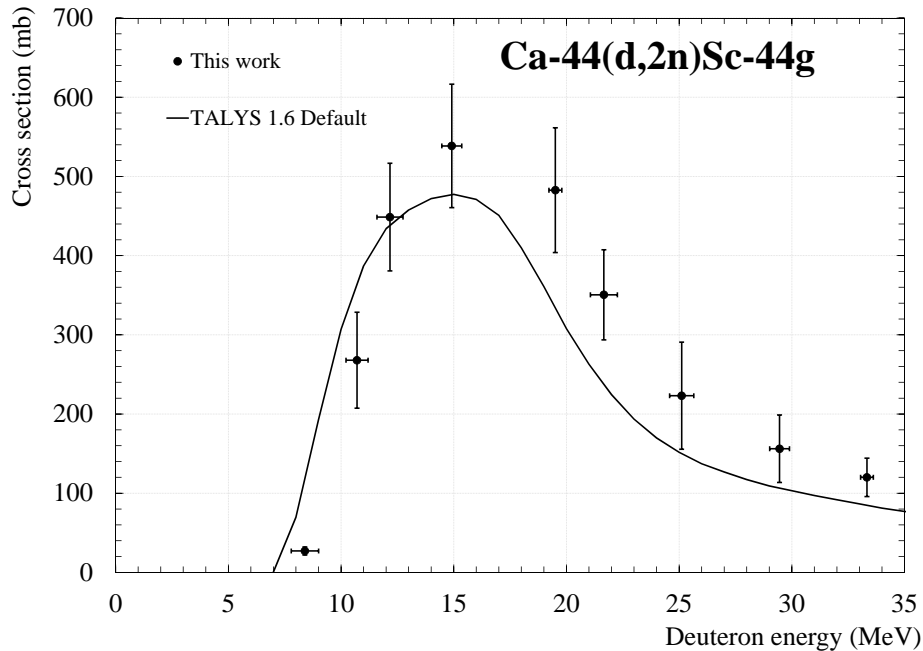
Figure 4: Excitation function for the Ca-44(d,2n)Sc-44g reaction (direct production)

3.1.3. Production cross section of K-42

K-42, with a half-life of 12.260 (3) hours, decays by β- process (100 %) to Ca-42 (stable). It emits one main γ ray at 1524.7 keV with a branching ratio of 18 %. This gamma line has been used to determine the K-42 activity and deduce its production cross section, plotted in figure 5. The K-42 activity has not been obtained for all energies as it was not the main objective of this study. The TALYS code is not able to reproduce the excitation function for this reaction.

3.1.4. Production cross section of K-43

K-43 has a half-life of 22.3 (1) hours and decays by β- emission at 100 % to Ca-43 (stable), emitting four gamma rays with a branching ratio higher than 11 % (see Table 3). Among these gammas, one is common to Sc-43. The three others gamma lines have been used to extract the cross section values. They also have permitted to deduce the K-43 contribution in the gamma line (372.9 KeV), which is common with Sc-43. In figure 6, we can see that our experimental data are in agreement with the reaction energy threshold at 15.07 MeV. The TALYS code is not able to reproduce the experimental
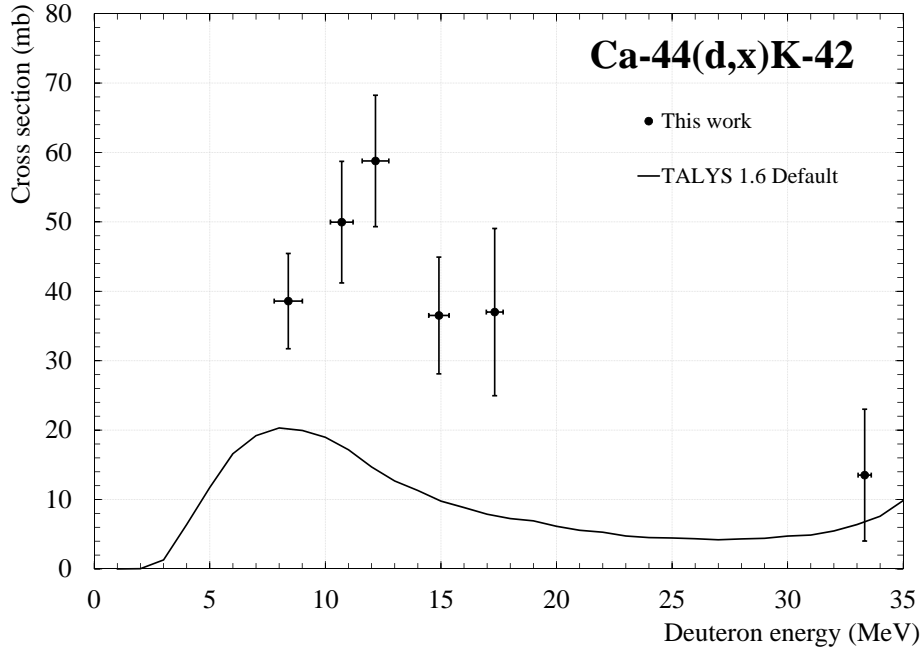
Figure 5: Excitation function for the Ca-44(d,x)K-42 reaction

trend and amplitude for this reaction.

3.1.5. Production cross section of Sc-43

The Sc-43 has a half-life of $T_{1/2} = 3.891$ (12) h. It is a 88 % $\beta+$ emitter and decays to Ca-43 (stable), by emitting a γ ray at 372.9 keV (see Table 3) with a branching ratio of 22.5 %. This gamma line is common with K-43 which is also produced in the target (see part 3.1.4).

The activity of Sc-43 has been deduced from this peak using the other detectable gammas emitted by K-43, resulting on an additional uncertainty source for the determination of Sc-43 activity. As there is some cooling time of 14 hours between the end of irradiation and the activity measurements, the short half-life of Sc-43 and its low production cross section, don't permit to detect Sc-43 in every irradiated target. When the activity was high enough to be detected, the uncertainty on the peak fit was up to 30 %. Only two cross section values at 21.66 and 33.33 MeV were measured and are reported in Table 4. These values are plotted in figure 7 with the results of the TALYS code with default parameters. As no experimental data are available around the maximum plotted by TALYS, the amplitude of the curve can not be ver-
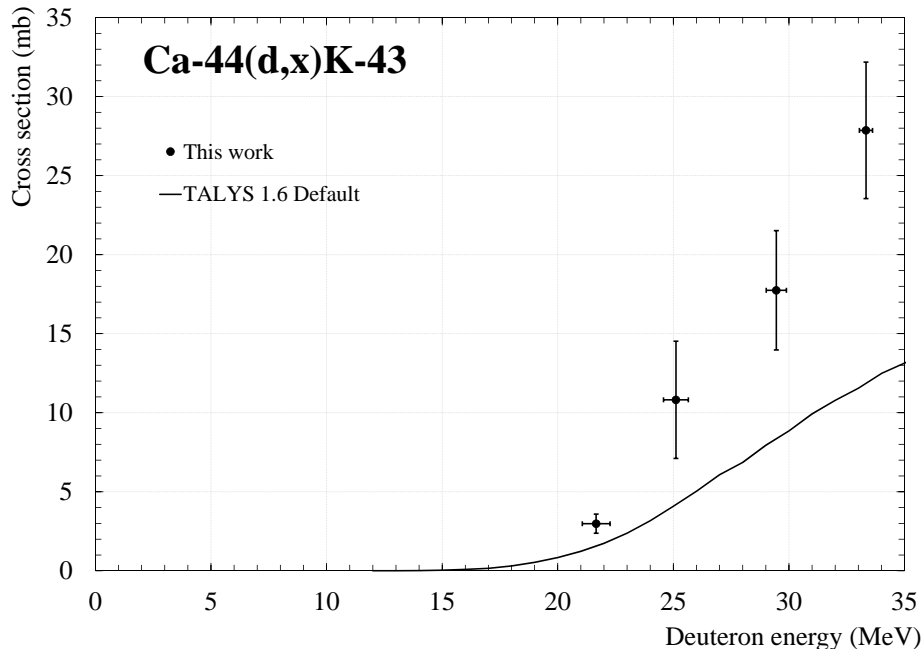
15

Figure 6: Excitation function for the Ca-44(d,x)K-43 reaction

ified. However, our existing experimental data points are in good agreement compared to the TALYS values. In addition, the Sc-43 is produced by a (d,xn) as well as Sc-44 for which the TALYS code shows a good reproduction of the trend.

3.2. Thick Target production Yield of Sc-44

Sc-44 can be produced using Ca-44 with protons or deuterons as projectiles. The Thick Target production Yields of Sc-44g and Sc-44m using deuterons have been obtained from the experimental production cross sections determined in this work. They are plotted in figures 8 (a) and (b), respectively. These data are compared with the proton route, calculated from results summarized in databases (National Nuclear Data Center).

Using protons as projectiles at 30 MeV, the Sc-44g TTY calculated from the experimental cross section values of Mitchell et al., 1982, Levkovskij, 1991 and Krajewski et al., 2013, is 2.7 GBq/μA.h (see figure 8 (a)). In this work, we calculate from our new cross section values obtained with deuterons a TTY of 2.9 GBq/μA.h at 30 MeV, which is close to the value calculated in the case of protons. The cross section values obtained with the TALYS

16
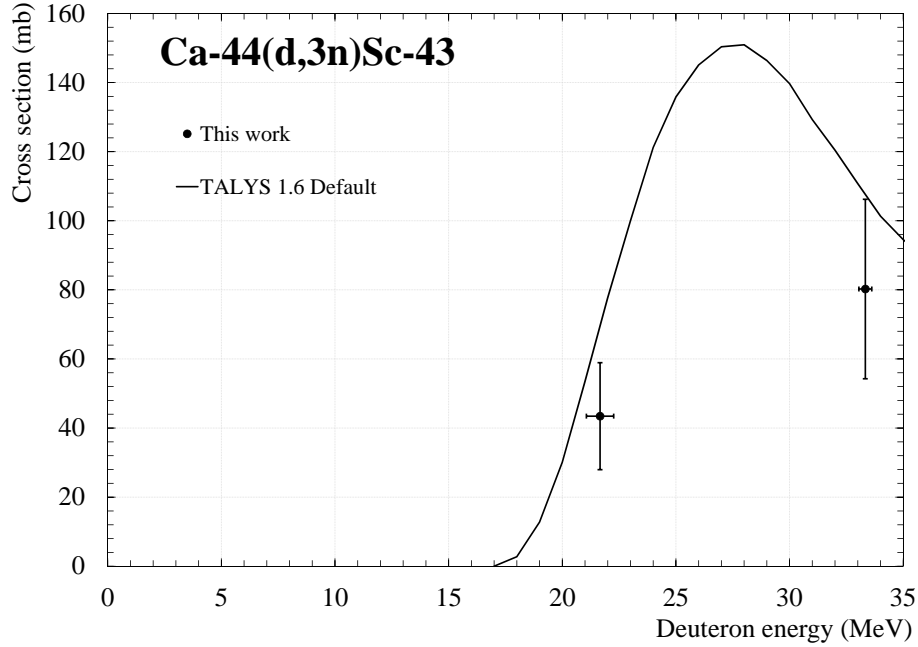
Figure 7: Excitation function for the Ca-44(d,3n)Sc-43 reaction

code lead to a TTY of 2.3 GBq/μA.h (figure 2 (a)), i.e. 21 % lower than the experimental value.

For the production of Sc-44m, the TTY is 23 MBq/μA.h with protons at 30 MeV (see figure 8 (b)). From our data using deuterons, the TTY is 70 MBq/μA.h with the same incident energy i.e. 3 times higher than the one obtained with protons. With the TALYS code results, the TTY is calculated to be 65 MBq/μA.h, 7% lower than the experimental one.

These results show that higher Sc-44g production rate is obtained using protons instead of deuterons up to 27 MeV. With 30 MeV protons and deuterons, similar amount of Sc-44g is produced with 2.7 and 2.9 MBq/μA.h, respectively. It must be taken into account that a smallest amount of carbonate calcium material is necessary with deuterons at 30 MeV as compared to protons with the same energy. Indeed, the target thickness has to be 2.3 mm using deuterons against 4.1 mm using protons. In addition, the production of Sc-44m can significantly be increased using deuterons as projectiles instead of protons.

3.3. Sc-44 production scenarios

Three production scenarios can be set and are presented below, depending of the use of Sc-44 and the cyclotron characteristics of commercially available machine (15 MeV, 30/15 MeV and 70/35 MeV proton/deuteron).

3.3.1. Production of Sc-44g for conventional PET imaging with small vector molecule

The first scenario is the production of scandium-44g for conventional PET imaging for which Sc-44m has to be limited. Sc-43 is also of interest for PET and emits positrons with energies close to those of Sc-44g. Avoiding the production of Sc-43 is not an issue for this production scenario. The figure 8 (b) shows that the production of Sc-44m with protons is lower than with deuterons on the whole investigated energy range. This way, the use of protons is the best choice, compared with deuterons, to produce Sc-44g for PET imaging.

3.3.2. Production of Sc-44g for the new 3 γ imaging technique

The second scenario is the production of scandium-44g for the new 3 gamma imaging technique using peptide or small molecule with rapid distribution on the body. In this case, Sc-44g is the radionuclide to produce in high quantity. The Sc-44m and Sc-43 production are not necessary as they don't have the third high energy γ required for this new diagnosis technique. They will add noise on the detection system and an additional unnecessary dose to the patient. Sc-44m and Sc-43 can not be separated from Sc-44g in the target, contrary to the potassium isotopes (see figure 5 and figure 6).

With a 15 MeV proton cyclotron. As shown in figure 8 (a), 1.9 GBq/μA.h of Sc-44g is directly produced with 15 MeV protons. The figure 9 shows the Sc-43 TTY calculated for protons as projectiles using the values published by Levkovskiy, 1991, and for deuterons using the TALYS 1.6 Default values plotted in figure 7. Irradiating the target with a 15 MeV proton beam leads to a Sc-43 production yield of 2.4 MBq/μA.h and 10.5 MBq/μA.h for Sc-44m (see figure 8 (b)). For these conditions of irradiation, the Sc-43 and Sc-44m production yields at the end of irradiation represent, respectively, 0.1 % and 0.6 % of the Sc-44g activity directly produced.

With a 30 MeV proton - 15 MeV deuteron cyclotron. With 15 MeV deuterons, the amount of Sc-44g produced in the calcium-44 carbonate target is 680

MBq/μA.h (see figure 8 (a)). For this energy, no Sc-43 can be produced as the Ca-44(d,3n)Sc-43 reaction threshold is 17.1 MeV. 11 MBq/μA.h of Sc-44m will be produced (see figure 8 (b)) which is 1.6 % of the Sc-44g activity. With 30 MeV protons, 2.7 GBq/μA.h of Sc-44g is produced. The production yield of Sc-43 is 1.2 GBq/μA.h (see figure 9) and 23 MBq/μA.h for Sc-44m, which represent respectively 44 % and 0.9 % of the Sc-44g activity.

With a 30 MeV deuteron cyclotron. With 30 MeV deuteron, the Sc-44g TTY is 2.9 GBq/μA.h, close to that obtained with 30 MeV protons. The amount of Sc-44m and Sc-43 produced are, respectively, 70 MBq/μA.h and 600 MBq/μA.h. This corresponds to 2.4 and 20.7 % of Sc-44g activity.

3.3.3. Production of the Sc-44m/Sc-44g in-vivo generator for antibody labelling

The last scenario is about the production of the in-vivo generator Sc-44m/Sc-44g for antibody labelling. A study has shown that the Sc-44m/Sc-44g generator labelled with a DOTA-peptide is chemically stable and that Sc-44g stays attached to the chelator after the decay of its parent radionuclide Sc-44m (Huclier-Markai et al. in 2014). The in-vivo generator permits to extend the Sc-44 lifetime in the patient body. Sc-44m can then be used for antibody labelling for both conventional PET and 3 γ imaging. For this purpose, Sc-43 and Sc-44g direct production are useless since the transit time of antibodies is long as compared to their half-live.

The figure 10 shows that the Sc-44m/Sc-44g cross section ratio (a) and the Sc-44m/Sc-44g TTY ratio(b) are higher using deuterons instead of protons.

In the specific case where an in-vivo generator Sc-44m/Sc-44g is used, a deuteron beam has to be prefered.

From a 15 MeV deuteron beam, no Sc-43 can be produced and 680 MBq/μA.h of Sc-44g is produced. The Sc-44m TTY for this energy is 11 MBq/μA.h. It is 62 times less than the Sc-44g activity.

With 30 MeV deuteron beam, 70 MBq/μA.h of Sc-44m is produced. The figure 11 shows the decay of Sc-44m, Sc-44g and Sc-43 taking into account the initial activity produced with a 30 MeV deuteron beam. The secular equilibrium between Sc-44m and Sc-44g is reached after 50 hours, which is close to one Sc-44m half-life, i.e. 2.44 days. Waiting for this time after the end of irradiation, the Sc-43 production decreases to 18 kBq/μA.h (0.05 % of Sc-44m activity) and the Sc-44g direct production decreases to 2.3 kBq/μA.h.

The Sc-44m production, waiting for 2.44 days after the end of irradiation reaches 35 MBq/μA.h, which is 3.2 times higher than the one obtained with 15 MeV deuterons at the time of the end of irradiation.

However, only few accelerators in the world are able to deliver 30 MeV deuterons, but the technology is available. This type of cyclotron permits to produce a higher amount of Sc-44m than using 15 MeV deuterons or a proton beam.

4. Conclusion

New experimental cross section values have been presented for the Ca-44(d,x)Sc-44m, Sc-44g reactions with some informations on the Sc-43, K-42 and K-43 contaminants. The TALYS results are close to experimental values for the Ca-44(p,n) and Ca-44(d,2n) reactions. New measurements dedicated to Sc-43 with deuterons as projectiles are needed to obtain experimental values on this contaminant production cross section, and validate, or not, the trend made by the TALYS code. However, TALYS with default models is not able to reproduce the data for the production of potassium isotopes.

These new sets of experimental data allow to calculate Thick Target production Yields and compare the proton and deuteron routes for three different Sc-44 production scenarios. This article shows that the use of proton beam is the best choice, as compared to deuterons, to produce Sc-44g for PET imaging using peptide or small molecules with rapid distribution in the body. For the new 3 γ imaging technique developed at the SUBATECH laboratory, Sc-44g has to be produce with protons of 15 MeV to limit background generated by the Sc-44m and Sc-43 decay.

The production of the Sc-44m/Sc-44g in-vivo generator for antibody labelling required the highest Sc-44m production rate, with a limited amount of Sc-44g directly produced. Our new experimental results have shown that the Sc-44m/Sc-44g cross section and TTY ratios are higher with deuterons than with protons, whatever the incident beam energy. The production of Sc-44m for the in-vivo generator is advantageous with deuterons as projectiles, using a calcium-44 carbonate target. Sc-44m can be produced with 15 MeV deuterons beam but a higher amount of Sc-44m is produced with a 30 MeV deuteron beam. With this last energy value, some cooling time before the extraction and separation processes permits to better reduce the contribution of directly produced Sc-44g activity and obtain, by the way, a negligible level of Sc-43.
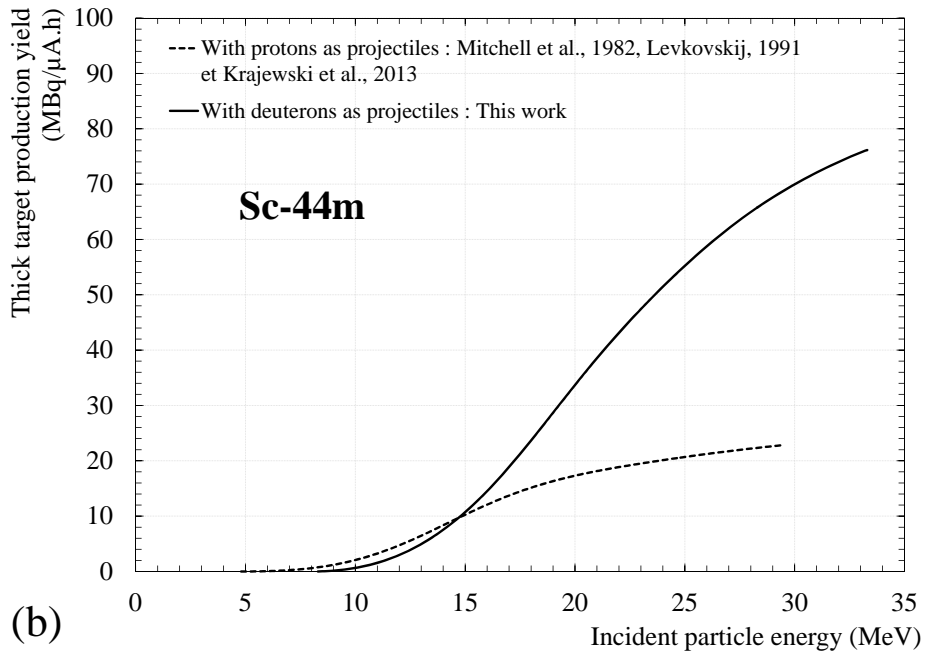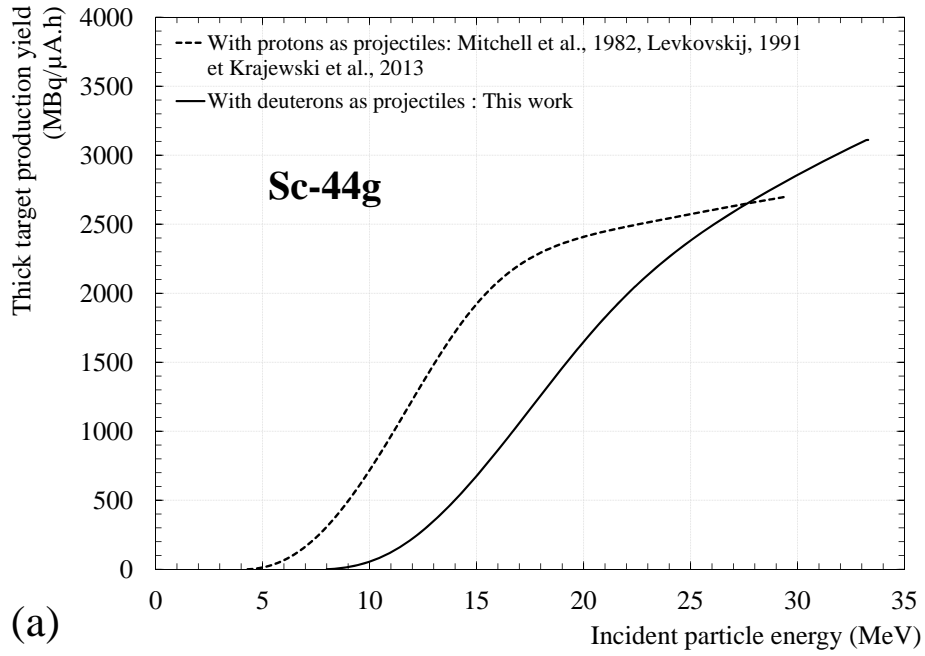
5. Acknowledgments

Figure 8: Thick Target production Yields for the Ca-44(d,2n)Sc-44g (a) and Ca-44(d,2n)Sc-44m (b) reactions, calculated with the cross section values of this work. Comparison with the Ca-44(p,n)Sc-44g (a) and Ca-44(p,n)Sc-44m (b) reactions.

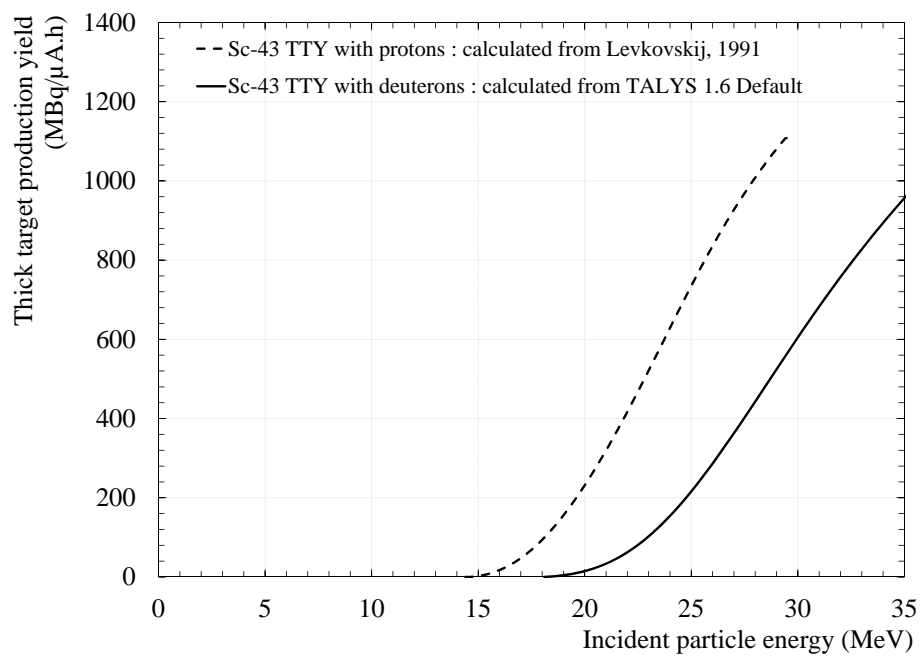Figure 9: Thick Target production Yields for the Ca-44(d,3n)Sc-43 and the Ca-44(d,2n)Sc-43 reactions, calculated with the cross section values of levkovskij, 1991 for the proton route and with the TALYS 1.6 Default results for the deuteron route
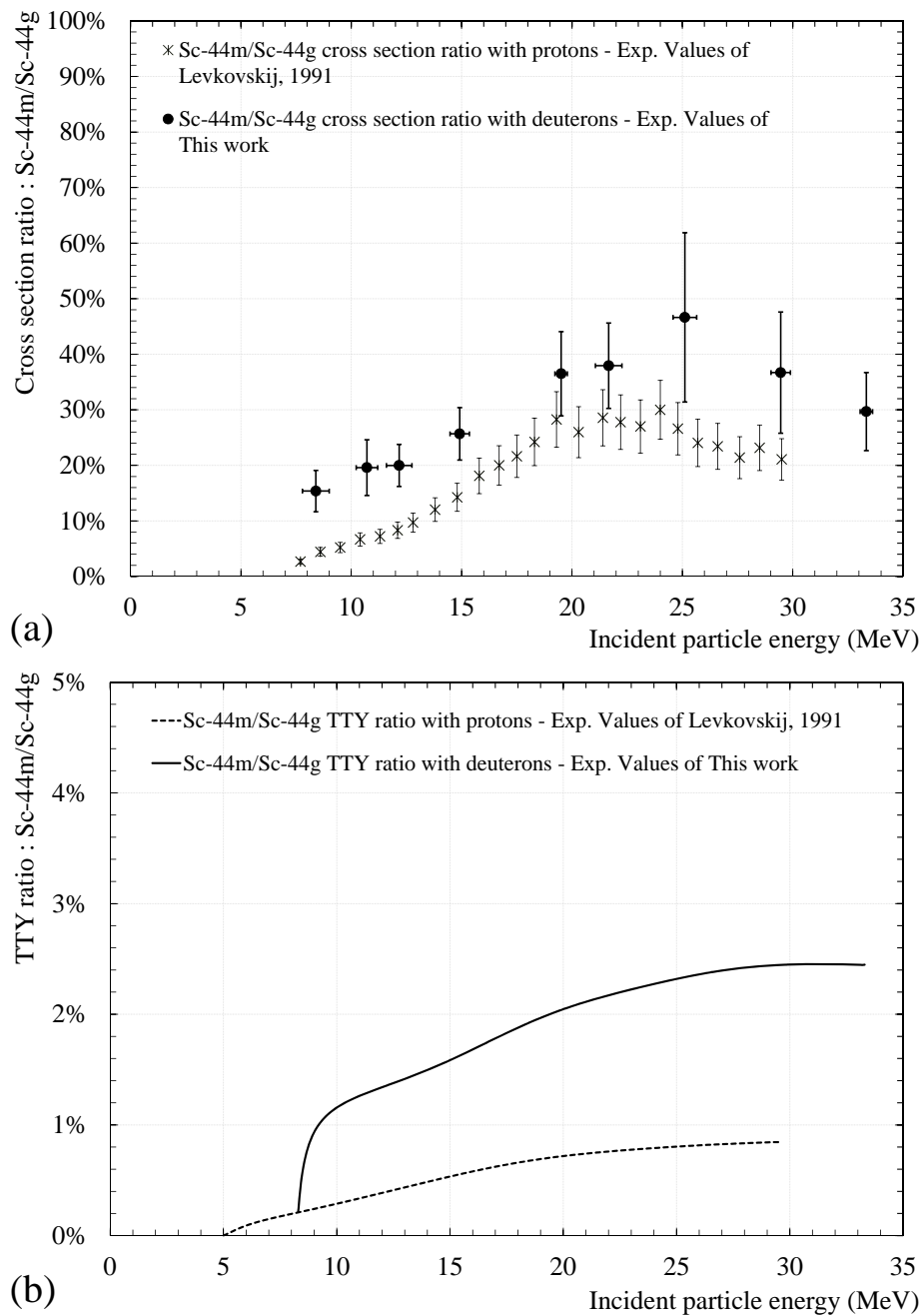
Figure 10: Experimental Sc-44m/Sc-44g cross section (a) and calculated TTY (b) ratios using protons and deuterons as projectiles
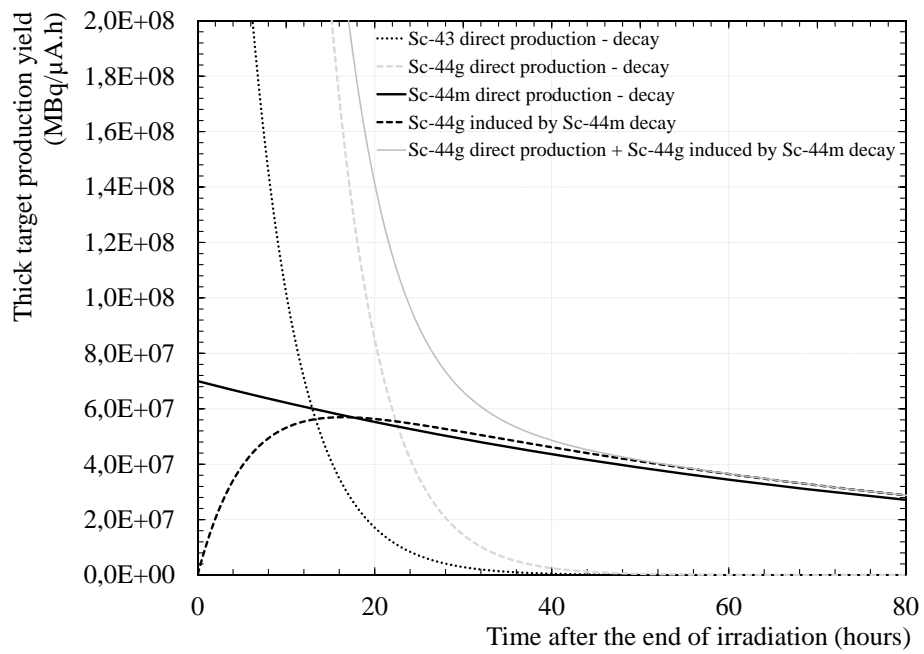
Figure 11: Sc-44m, Sc-44g and Sc-43 decay from an initial activity produced with a 30 MeV deuteron beam

Table 3: Produced radioisotope parameters (National Nuclear Data Center; Ekström and Firestone, 2004)

Radioisotope	$T_{1/2}$ (hours)	E_γ(keV)	I_γ(%)	Contributing reaction(s)	Threshold (MeV)
Sc-44m	58.6 (1)	271.13	86.7 (3)	Ca-44(d,2n)	7.23
Sc-44g	3.927 (8)	1157.031	99.9	Ca-44(d,2n)	6.96
Sc-43	3.891 (12)	372.76	23	Ca-44(d,3n)	17.11
K-42	12.360 (3)	1524.7	18	Ca-44(d,α)	0.00
				Ca-44(d,2p+2n)	25.13
K-43	22.3 (1)	372.76	23	Ca-44(d,d+p)	12.74
		396.861	11.85 (8)	Ca-44(d,2p+n)	15.07
		593.390	11.26 (8)		
		617.490	79.2 (6)		

Table 4: Experimental cross section values (mb) for Ca-44(d,2n)Sc-44m,Sc-44g, Ca-44(d,3n)Sc-43 and Ca-44(d,x)K-42,K-43 reactions

Energy (MeV)	σ Sc-44m (mb)	σ Sc-44g (mb)	σ Sc-43 (mb)	σ K-42 (mb)	σ K-43 (mb)
33.33 ± 0.28	35.63 ± 4.42	120.05 ± 24.25	80.25 ± 25.98	13.51 ± 9.50	27.86 ± 4.32
29.45 ± 0.44	57.29 ± 6.74	156.12 ± 42.62			17.74 ± 3.77
25.11 ± 0.54	104.01 ± 12.71	223.06 ± 67.61			10.82 ± 3.71
21.66 ± 0.60	132.97 ± 16.14	350.52 ± 56.88	43.44 ± 15.49		2.98 ± 0.61
19.51 ± 0.29	176.10 ± 22.53	482.57 ± 78.80			
17.33 ± 0.36	184.46 ± 25.73			37.00 ± 12.05	
14.91 ± 0.44	138.25 ± 15.76	538.49 ± 77.97		36.52 ± 8.41	
12.17 ± 0.58	89.64 ± 10.26	448.59 ± 67.96		58.78 ± 9.47	
10.71 ± 0.49	52.49 ± 6.37	267.88 ± 60.57		49.96 ± 8.76	
8.40 ± 0.61	4.16 ± 0.63	27.05 ± 5.09		38.59 ± 6.87	

6. References

Alliot, C., Audouin, N., Barbet, J., Bonraisin, A.C., Bossé, V., Bourdeau, C., Bourgeois, M., Duchemin, C., Guertin, A., Haddad, F., Huclier-Markai, H., Kerdjoudj, R., Laizé, J., Métivier, V., Michel, N. and Mokili, M., 2015. Is there an interest to use deuteron beams to produce non-conventional radionuclides?, Frontiers in Medicine doi: 10.3389/fmed.2015.00031.

Blessing, G., Bräutigam, W., Böge, H.G., Gad, N., Scholten, B., and Qaim, S.M., 1995. Internal irradiation system for excitation function measurement via the stacked-foil technique, Appl. Radiat. Isot. 955, 46-9.

Chemgas®, major supplier of enriched stable isotopes: http://www.chemgas.com/

Duchemin C., Guertin A., Haddad F., Michel N. and Métivier V., 2015. Cross section measurements of deuteron induced nuclear reactions on natural tungsten up to 34 MeV, Applied Radiation and Isotopes 97 (2015) 52-58

Duchemin C., Guertin A., Haddad F., Michel N. and Métivier V., 2015. Production of medical isotopes from a thorium target irradiated by light charged particles up to 70 MeV, Phys. Med. Biol. 60, 931-946.

Durnez A., Petitbon-Thévenet V. and Fortuna F., 2014. Preparation of molybdenum target by centrifugal method, J. Radioanal. Nucl. Chem. 299:1149-1154.

Ekström, L.F., and Firestone, R.B., 2004. Information extracted from the Table of Radioactive Isotopes, version 2.1.

FitzPeaks Gamma Analysis and Calibration Software version 3.66, produced by JF Computing Services (UK), based on methods presented in Nucl.Instrum. and Methods (1981) 190, 89-99, describing the program SAMPO80 of the Helsinki University of Technology, Finland.

Gallego Manzano, L., Bassetto, S., Beaupere, N., Briend, P., Carlier, T., Chérel, M., Cussonneau, J-P., Donnard, J., Gorski, M., Hamanishi, R., Kraeber-Bodéré, F., LeRaya, P., Lemaire, O., Masbou, J., Mihara, S., Morteau, E., Scotto Lavina, L., Stutzmann, J-S., Tauchi, T., Thers, D., 2014. XEMIS: A liquid xenon detector for medical imaging, Nuclear Instruments and Methods in Physics Research A, doi:10.1016/j.nima.2014.11.040.

Grignon C., Barbet J., Bardies M., et al. (2007). Nuclear medical imaging using beta+ gamma coincidences from Sc-44 radio-nuclide with liquid xenon as detector medium, Nucl. Instrum. Meth. A 571, 142-145.

Haddad, F., Ferrer, L., Guertin, A., Carlier, T., Michel, N., Barbet, J., Chatal, J.F., 2008. Arronax a high-energy and high-intensity cyclotron for nuclear medicine, Eur. J. Nucl. Med. Mol. Imaging 35, 1377-1387.

Huclier-Markai S., Kerdjoudj R., Alliot C., Bonraisin A.C., Michel N., Haddad F., Barbet J., 2014. Optimization of reaction conditions for the radiolabelling of DOTA and DOTA-peptide with 44m/44Sc and experimental evidence of the feasibility of an in vivo PET generator. Nuclear Medicine and Biology 41, e36-e43.

Koning, A.J., Rochman, D., 2012. Modern nuclear data evaluation with the TALYS code system, Nucl. Data Sheets 113, 2841.

Krajewski, S., Cydzik, I., Abbas, K., Bulgheroni, A., Simonelli, F., Holzwarth, U., Bilewicz, A., 2013. Cyclotron production of 44Sc for clinical application, Radiochimica Acta, Vol.101, p.333.

Levkovskij, V.N, 1991. Activation cross section nuclides of average masses (A=40-100)by protons and alpha-particles with average energies (E=10-50 MeV)., Reference Book: Levkovskij,Act.Cs.By Protons and Alphas,Moscow 1991.

Majkowska-Pilip A. and Bilewicz A., 2011. Macrocyclic complexes of scandium radionuclides as precursors for diagnostic and therapeutic radiopharmaceuticals. J. Inorg. Biochem., 105.

Mitchell L.W., Anderson M.R., Kennett S.R., and Sargood D.G, 1982. Cross sections and thermonuclear reaction rates for 42Ca(p,)43Ca, 44Ca(p,) 45Sc, 44Ca(p,n) 44Sc and 45Sc(p,n)45Ti. Nuclear Physics A, 380.

Müller C., Bunka M., Haller S., Köster U., Groehn V., Bernhardt P., Van der Meulen N., Türler A., and Schibli R., 2014. Promising prospects for 44Sc- /47Sc-based theragnostics : Application of 47Sc for radionuclide tumor therapy in mice. J Nucl Med, 55.

National Nuclear Data Center, information extracted from the Experimental Nuclear Reaction Data (EXFOR) Database, http://www.nndc.bnl.gov/exfor/exfor.htm, Version of November 05, 2013.

Oger T. et al., 2012. A liquid xenon tpc for a medical imaging compton telescope, Nucl.Instrum.Meth. A, 695.

Petitbon-Thévenet V., 2010. The target manufacturing laboratory at the IPNO, Target and Stripper Foil Technologies for High Intensity Beams - Proceedings of the 24th World Conference of the International Nuclear Target Development Society, Nuclear Instruments and Methods in Physics Research Section A: Accelerators, Spectrometers, Detectors and Associated Equipment, Volume 613, Issue 3, Pages 419-422.

Roesch F. et al., 2012. Scandium-44: benefits of a long-lived PET radionuclide available from the (44)Ti/(44)Sc generator system., Curr Radiopharm., 5(3):187-201.

Tárkányi, F., Takács, S., Gul, K., Hermanne, A., Mustafa, M.G., Nortier, M., Oblozinsky, P., Qaim, S.M., Scholten, B., Shubin, Yu.N., Youxiang, Z., 2001. Beam monitor reactions, in Charged Particle Cross Section Database for Medical Radioisotope Production: Diagnostic Radioisotopes and Monitor Reactions; IAEA-TECDOC-1211, pages 49-152, IAEA, Vienna. Database available on https://www-nds.iaea.org/medportal/, update may 2013.

Tárkányi, F., Sonck, M. and Hermanne, A., 2002. Investigation of the natMo(p,x)96mgTc nuclear reaction to monitor proton beams: New measurements and consequences on the earlier reported data, Nuclear Instruments and Methods B 198, 183.

Ziegler, J.F., Ziegler, M.D. and Biersack, J.P., 2010. SRIM The stopping and range of ions in matter, Nucl. Instrum. Methods Phys. Res., Sect. B 268, 1818-1823.